Full-scale pressure measurements on a Sparkman and Stephens 24-foot sailing yacht

Viola, I.M., Flay, G.J.F.

Full-scale pressure measurements on a Sparkman and Stephens 24-foot sailing yacht

J. Wind Eng. Ind. Aerodyn. 98 (2010) 800–807.
doi:10.1016/j.jweia.2010.07.004

Abstract

The aerodynamics of a Sparkman and Stephens 24-foot sailing yacht was investigated. Full-scale pressure measurements were performed on the mainsail and the genoa in upwind condition. Pressure taps were adopted to measure the pressures on three horizontal sections on the windward and leeward sides of the two sails. Several trims and apparent wind angles were tested. The present paper shows the pressure distributions on the sails and correlates the measured pressures with the flow pattern. In particular, leading-edge laminar separation bubble, turbulent reattachment and turbulent separation are discussed. Pressure measurements are also adopted to draw some trim guidelines.

1. Introduction

Sail aerodynamics has been widely investigated in the last half century and it is common practice to characterize it by aerodynamic force components, whilst pressure on sails is rarely measured.

Forces are commonly measured at model-scale in wind tunnels. Boundary-layer wind tunnels are designed to model the atmospheric boundary-layer, and special devices allow the vertical wind profile to be twisted to model the twisted flow resulting from the sum of the atmospheric boundary layer and the boat speed in full-scale. The yacht model is placed onto a balance, which allows the aerodynamic forces to be measured. The sails are flexible to allow several sail trims to be investigated. Various sail shapes, yacht heels, apparent wind angles, etc, are tested to investigate the relationship between different geometries and the aerodynamic forces.

One of the main limitations of wind tunnel tests is the inability to reach full-scale Reynolds number. In fact, most of the wind tunnels used for yacht testing do not allow wind speeds larger than 10 m/s and model-scales larger than $1/10^{th}$. The wind speed in full-scale is between 3 and 15 m/s and hence, the model-scale wind-speed should be between 30 and 150 m/s in order to match full-scale Reynolds numbers. This exceeds the maximum speeds achievable. Moreover, sails are thin membranes, which would not support the aerodynamic loads of a 30 m/s air speed.

Pressures on sails have rarely been measured either in model-scale or in full-scale. In model-scale, pressure measurements are complicated because sails are flexible in order to be trimmed, the weight of the pressure transducers affects the sail shape, and the dimension of the transducer affects the flow field. When solid and thick sails are adopted to support the transducer weight, the sails can only be trimmed with difficulty.

In full-scale, pressure measurements are complicated because of the unsteady wind environment and the large number of parameters involved. The atmospheric boundary layer is fully turbulent and does not usually provide a steady wind environment. The sails are flexible and the shapes change with the wind speed. The boat heels and pitches continuously due to the waves and the wind.

The differential pressure across a sail is 3 orders of magnitude smaller than the absolute value of the pressure. In fact, atmospheric pressure is between 95,000 Pa and 105,000 Pa, whilst the differential pressure across sails is of the order of magnitude of the dynamic pressure, which is roughly 15 Pa in a 5 m/s wind. Hence, the required accuracy of the pressure instrumentation is of the order of magnitude of one Pascal. To increase the accuracy, the differential pressure across the sail instead of the absolute pressure is measured.

If the pressure distributions on the windward and leeward sides of the sail need to be measured individually (instead of only the differential values between the two faces), a reference pressure is necessary. In particular, to relate the pressures with the test conditions, the undisturbed far field conditions should be chosen as the reference static and dynamic pressure. Ideally, a differential pressure transducer should be connected through pressure tubes to the far field and to the sail. Because this is impossible, a stable reference pressure, possibly representative of the far field pressure, should be found somewhere onboard the vessel.

With regard to the static far-field pressure, the following two remarks should to be considered. An incoming atmospheric disturbance can change the atmospheric pressure by several Pascal per minute. Hence, the far field pressure can change significantly during the acquisition period. Moreover, the vertical pressure gradient due to hydrostatic effects is of the order of 10 Pa/m. Hence, on a 10 m high mast, the static pressure at the top of the sail is roughly 100 Pa larger than the pressure at the bottom of the sail height.

With regard to the dynamic far-field pressure, the following two remarks should to be considered. The differential pressure across the sail varies linearly with the dynamic pressure and thus with the square of the wind speed. Hence, when a gust increases the wind speed by 1m/s, the dynamic pressure increases by roughly 5 Pa. Moreover, the dynamic pressure is higher at the highest sail sections than at the lowest sail sections, due to the atmospheric boundary layer.

The difficulties above were overcome in the present paper, which discuss the pressure distributions on the sails of a 24-foot sailing yacht. Differential pressures were measured, with the reference pressure being the pressure inside the yacht cabin, which was supposed representative of the far field static pressure. The reference dynamic pressure was measured with Pitot static probes located at several locations onboard. The pressure on three horizontal sail sections of the mainsail and genoa were measured for different sail trims.

The present paper shows the pressure distribution on a typical modern sail-plan measured with a state-of-the-art measuring system. Pressure distributions on sails have been rarely published, particularly in full scale. As far as known by the present authors, the only published full-scale measured pressure distribution was presented by Warner & Ober in 1925. The innovative contributions in the present paper are the larger number of pressure transducers used, which allow a high-resolution map of the sail pressure distributions; the high resolution of the transducers, which allows small pressure differences due to the sail trim to be measured; the high sampling frequency, which allows mean values taking into account the high frequency fluctuations to be measured accurately.

The design of high-performance sails is performed with numerical methods, which compute aerodynamic forces. Several candidate sails are processed, and a Velocity Prediction Program (VPP) uses the aerodynamic forces to compute the boat speeds achieved with each candidate sail, Pressure distributions and the aerodynamic forces are computed numerically and are not measured. Indeed, complicated phenomena are involved, such as the laminar to turbulent transition, leading edge separation and reattachment, and the trailing edge separation, which are all modelled with difficulty. Therefore, experimental validation is essential to check on the numerical modeling accuracy. Wind tunnel measurements are often used to validate the numerical computations; but wind tunnel modelling does not take into account the lowest frequency components of the atmospheric boundary-layer turbulence and the yacht dynamics. Moreover, the model-scale Reynolds number that can be achieved in wind-tunnel testing is one order of magnitude lower than the full-scale Reynolds number. Therefore, full-scale pressure measurements, such as the present measurements, have to be used to validate the numerical methods.

2. State of the Art

Until the beginning of the last century, the aerodynamics of sailing yachts was described by empirical formulae. For instance, Skene (1938) quoted the “Martin’s Formula” $p=0.004 \cdot U^2$ giving the mean pressure load “p” (in pounds per square foot) on the sails due to the wind speed “U” (in miles per hour).

During the first half of the last century, yacht builders and designers such as the Herreshoff family, and Sparkman & Stephens, turned wind tunnels and towing tanks into essential tools for yacht design. Unfortunately, a collection of their research is unknown to the authors.

Between 1915 and 1921, Warner & Ober performed several experiments at the Massachusetts Institute of Technology (MIT) to find the relationship between the performance of the sails of a yacht compared to the wings of an airplane and in 1923 they performed the first full-scale pressure measurements on the S-class yacht *Papoose* (Warner & Ober 1925). They measured the pressure with manometers connected to three sections of the mainsail and one section of the jib, and investigated the difference between a mainsail with and without battens, and the effect of one sail on the pressure distribution of the other sail.

In the early 1960s, Marchaj (1964) measured with manometers the pressure on eight sections of a model-scale mainsail in the University of Southampton Wind Tunnel.

In the 1970s, Gentry (1971) was interested in the slot effect due to jib/mainsail interaction and investigated the pressure distributions with an Analogue Field Plotter on a 2D model. He was involved in the design of the masts for the successive America’s Cup defences Courageous, Freedom and Liberty in the 1974 and 1977, 1980, 1983 America’s Cup defences respectively (Gentry 1988). The pressure distribution on the mast/mainsail was investigated with the CFD code of the Boeing Commercial Airplane Company.

In the 1980s, Wilkinson (1984, 1989, 1990) studied mast/sail interaction on a 2D model-scale section. After these few authors, pressure measurements on sails have rarely been published.

Over the past 3 years, full-scale measurements have made a resurgence and new lightweight small devices have allowed better measurements to be taken. The Yacht Research Unit (YRU) at the University of Auckland is developing a wireless pressure system for full-scale experiments (Flay & Millar 2006), and similar systems were also developed by an Italian research team (Puddu *et al.* 2006) and by an American team collaborating with the America's Cup challenger BMW Oracle Racing (Graves *et al*. 2008). At the current state of the art, these systems have provided pressure measurements at only a few points and have not yet been able to provide a complete pressure map on sails.

In the past year at the YRU wind tunnel, double-surface rigid sails with pressure tubes inside have been tested and the pressure distributions on both the windward and leeward sides of a fully 3D symmetrical spinnaker were measured (Richards & Lasher 2008). The pressures were measured with 8 pressure taps at each of 7 horizontal sections on a 1/25th model-scale International America's Cup Class (IACC) spinnaker sailing at an apparent wind angle (AWA) of 120°.

Finally, Viola & Flay (2010a and 2010b) measured a complete pressure map on the sail of a 1/15th model-scale AC33-class yacht sailing with mainsail and asymmetric spinnaker. Several trims of three sails, sailing at three AWAs and three heel angles were measured.

3. Full-Scale Pressure Measurement Experimental Setup

3.1 Description of Yacht

The yacht *Aurelie* was kindly provided for the experiment by Madame Emanuela Molinari Viola. The yacht is a Sparkman & Stephens 24-foot cruising yacht with a Bermuda rig, which was designed in the late 1960s by Sparkman & Stephens. She was built in New Zealand in 1978 in fibreglass and polyester resin, with an alloy mast and boom. Table 1 summarizes the main specifications of the Sparkman & Stephens 24'.

3.2 Sails

A mainsail with low roach (almost triangular) and a genoa with overlap were used. The fully-batten mainsail was brand new, whilst the genoa was older but in reasonable condition and without battens. Mean values of the sail section shapes were measured from photos taken during the experiments. The main dimensions of the sails are summarized in Table 2.

3.3 Pressure System

Surface pressures were measured on the sails with a system developed by the YRU. In particular, Nick Velychko developed the concept, the electrical circuit, the PCB layout, the enclosure design, and the LabVIEW control software, while David Le Pelley developed the LabVIEW data collection and manipulation software. The system has 512 channels, and each of them can acquire up to 3,900 samples per channel per second. The transducers have a pressure range of ±450 Pa and a resolution of 9.25 mV/Pa. All the transducers were pneumatically connected to a reference static pressure. The system is made of 4 boxes, which contain 64 transducers each. To simplify the measurement setup, only 42 transducers were used and hence, only one box was necessary. The box was connected to a laptop, which ran the acquisition software. A standard marine battery supplied 12 V DC to the pressure system. The pressure measurements were initially acquired at 1,000Hz for 5 minutes. Subsequent analysis of those data showed that high frequency signals were

damped by long tubes and hence, the sampling frequency was reduced to 100Hz to reduce the amount of stored data. It was also found that a recording duration of 120 seconds contained several periods of the lowest frequency fluctuations and hence, the subsequent data acquisitions were performed for 120 seconds.

This pressure system has also been used for the measurement of the complete map of the sail pressures on a 1/15th scale model of a AC33-class yacht sailing with mainsail and asymmetric spinnaker (Viola & Flay 2010a and 2010b).

The reference pressure was measured in a locker inside the yacht cabin, which was connected with a 10 m length tube to the box. The locker helped avoid that the static pressure measurement being affected by cabin ventilation. Each transducer was connected to a pressure tap through a tube, which was stuck onto the sails with adhesive tape. The pressure taps were truncated very flat cones with a base diameter of 20 mm and a height of 5 mm. The pressure tap on the top of the cone was connected to a stainless steel tube lying flat against the sail, to which the PVC pressure tube was connected. The pressure taps and the tubes were expected to be sufficiently small not to affect the sail boundary layer. In fact, the diameter of the pressure tube was of the same order of magnitude as the roughness of the sail, due to the cloth panel seams. However, to minimize the interference with the sail boundary layer, the tubes were stuck to the sail along the main flow direction in the region near the pressure taps. Figure 1 shows a schematic drawing of the acquisition system and a photograph of the pressure tap.

Pressure taps were placed on 3 horizontal sections of the two sails. To simplify the experiment, one sail face at a time was measured. Each test condition was repeated on both tacks. Hence, the same sail face was firstly the windward face and then the leeward face. To verify the correspondence of the test condition from one tack to the other, while measuring the pressure on one sail face, a few pressure taps were used to measure the pressure on the other face. Moreover, for each test, 4 pressure taps measured the pressures around the mast, two on the windward side and two on the leeward side respectively.

The measured genoa sections were at 1/4, 1/2 and 3/4 of the luff respectively, whilst the mainsail sections were at 1/4, 1/2 and 800 mm below 3/4 of the luff, respectively. The lowest section of the mainsail was chosen in order to be able to reach the pressure taps from the deck when the main was hoisted. On the top, middle and bottom sections, 6, 9 and 16 pressure taps were used, respectively. Figure 2 shows the sailplan of the yacht *Aurelie.* The figure shows the two sails with the three measurement sections, and the terminology adopted in the following description. In particular, the leading edge of the sail is also named the *luff*, while the trailing edge is named the *leech*; the aft (back) corner of the sails is connected to a rope named a *sheet* and is used to trim the sail; the *vang* is a rope used to increase the tension on the mainsail leech, and the *backstay* is a metal cable used to bend the top of the mast back by pulling on the top.

3.4 Reference Dynamic Pressure

Static and dynamic pressures were measured with three Pitot static tubes located on the windward side of the yacht. Two of them were fixed to the shrouds at two different heights. These were oriented approximately 35 degree to windward of the boat's heading. The third one was fixed on a pole, which held the probe roughly 1.5 m away from the boat stern on the windward side. This latter probe was free to pivot into the wind direction and was found

to be the most reliable of the three of them. The differential pressure between the total probe on the pole and the cabin reference static pressure was taken to be the reference dynamic pressure.

The measurements were performed in September 2009 in the Hauraki Gulf (Auckland, NZ), in roughly 4m/s of breeze. All the tests were performed sailing upwind, with AWAs between 25 and 45 degrees.

4. Results and Discussion

The pressures on the mainsail were measured for different mainsail and genoa trims. For each trim, the boat was sailed on the genoa trim using telltails, which means that the helmsman helmed the boat to keep the optimum course for the genoa trim. In this way, only optimum trims were tested. Hence, the AWA depended on the genoa trim.

The pressures on the genoa were investigated for different genoa trims. The effect of changing the angle of incidence of the genoa was investigated by sailing at a fixed AWA. This investigation allowed the optimum pressure distribution for a fixed AWA to be determined. Then, different AWAs were sailed and the genoa was trimmed according to each AWA.

The following results are shown in terms of pressure coefficients *Cp*, defined as the difference between the pressure measured on the sail surface *p* and the reference pressure inside the cabin p_∞, divided by the reference dynamic pressure *q* measured by the poled Pitot static tube. Note that the vertical axis is reversed in the following figures, showing negative values above and positive values below.

4.1 General Pressure Distribution Trend

A general trend of *Cp* along a sail section can be described. Figure 3 shows a schematic diagram of *Cp* along a generic section of the genoa and the mainsail. The correlated flow field is also shown. The apparent wind velocity *Va* is determined by the sum of the boat velocity *Vb* and the atmospheric true wind *Vt*.

The windward side of the two sails is a low speed region. Hence, *Cp* is near 1.0 over the whole section. The leeward side of the genoa shows a suction peak at the leading edge, which is followed by a quick pressure recovery with a local minimum suction at around 10% of the chord. The pressure recovery is related to the laminar separation bubble formed behind the sharp leading edge of the luff, which reattach after the turbulent transition (Abbot & Von Doenhoff 1949; Crompton & Barret 2000). The reattachment location is just in front of the local maximum pressure location (Crompton & Barret 2000). Downstream of the re-attachment, the pressure decreases again due to the section curvature, showing a second suction peak at a location between 20% and 40% of the curve length. After the pressure recovery, the pressure becomes constant due to the trailing edge separation (Thwaites 1969). The *Cp* variation over the genoa is similar to the *Cp* measured over the asymmetric spinnaker by the same authors in previous research (Viola & Flay 2010a and 2010b).

The leeward side of the mainsail shows similar trends to the genoa, but the laminar separation occurs on the mast, and the turbulent reattachment occurs at around 10% of the mainsail chord. Between the leading-edge suction peak and the pressure recovery due

to the reattachment, the pressure is almost constant. The *Cp* trends over the mainsail are in agreement with the measurements performed on a 2D mast/mainsail section by Wilkinson (1989).

4.2 Pressures on the Mainsail

Figure 4 shows the *Cp* over the three sections of the mainsail versus the position *x* along the chord *c*. The three curves are obtained with different trims of the mainsail sheet, which mainly changes the angle of incidence of the sail.

When the mainsail is tightened (trim #+1 in figure), the maximum differential pressure between the two sides is achieved. The *Cp* on the windward side is almost 1.0 over most of the chord, meaning it is a very low speed region. On the leeward side, the leading-edge suction peak reaches roughly *Cp*= -2 on the top section and *Cp*= -1 on the bottom section.

When the mainsail is eased (trim #0 in figure), the differential pressure between the windward and the leeward sides of the sails decreases. However, because easing the mainsail sheet decreases the angle of incidence but does not change the sail shape significantly, the second suction peak due to the sail curvature also does not change significantly. The windward *Cp* is lower showing a higher velocity on the windward side. The leading-edge suction on the leeward side decreases because of the decreased angle of incidence.

When the sail is eased even further (trim #-1 in figure), the angle of incidence becomes negative and the first 10% of the mainsail has negative *Cp*'s on the windward side and positive *Cp*'s on the leeward side.

The best trim depends on the wind conditions. In fact, from the figure it can be argued that by tightening the sheet, the pressure forces on the sail increase, resulting in higher thrust and side force components. In the tested condition, trim #0 allowed the highest boat speed. Trim #+1 resulted in excessive side force and hence, a higher heeling moment, which heeled the boat, increasing the hydrodynamic resistance.

Figure 5 shows the *Cp* over the three mainsail sections, for three mainsail twists. Twist was changed by tightening the leech, through the vang, the traveller and the sheet. On the top two sections, only the leeward-side pressure is plotted. The change in twist affects the *Cp* over only the highest sections, while the lowest section is insensitive to the twist. When the leech is tightened (from #-1 to #+1 in figure), the twist decreases and the angle of incidence of the highest sections increases. Therefore, on the highest section the leading-edge suction peak increases and trailing edge separation occurs, which causes the second suction peak to decrease. When the maximum leech tension is achieved (#+1), the flow is mainly separated, leading to an almost constant *Cp*. The low mean speed of the separated flow is unable to lift the tell-tails on the highest part of the mainsail leech,

From the figure, it can be argued that by increasing the leech tension the pressure force increases at the leading edge and decreases at the trailing edge, which rotates the direction of the resultant aerodynamic force further forward, leading to an increased thrust force and a reduced side force. However, increasing the leech tension also rotates the top sail-section backwards, which leads to the opposite effect. Therefore, the best trim is a medium trim, which maximizes the resultant thrust component. Moreover, by increasing

the leech tension, the aerodynamic load on the highest sections decreases which leads to a lower centre of effort.

Figure 6 shows the *Cp* over the three sections of the mainsail for three sail trims, where the effect of the size of the gap between sails is investigated. With regard to the reference trim (#0 in figure), firstly the mainsail was tightened and the genoa was eased, which increased the gap (#+1 in figure), then the mainsail was eased and the genoa was tightened, which decreased the gap (#-1 in figure). When the gap between the sails is increased, the *Cp* on the mainsail becomes constant along the three sections, showing a fully separated flow, which causes the leech tell-tails to collapse. In fact, easing the genoa leads to a lower downwash on the mainsail, which leads to a larger angle of incidence. Hence, when the mainsail was tightened and the genoa was eased, the mainsail stalled due to the excessive angle of incidence. Conversely, when the mainsail was tightened without easing the genoa (Figure 4, trim #+1), only the top section of the mainsail showed separated flow.

When the gap between sails is decreased (#-1), the lowest sections of the mainsail, where the genoa overlap is larger, show an inversion of pressure/suction between the windward/leeward sides of the sail. The mainsail stagnation point moves downstream on the leeward side of the mainsail. On the highest section, where the overlap is negligible, the *Cp* distribution shows the presence of a laminar separation bubble and hence, the stagnation point is at the leading edge and the angle of incidence is larger than the ideal angle of attack. Hence, the low angle of incidence at the lowest section is due to over-trim of the genoa and is not due to the mainsail trim.

Figure 7 shows the *Cp* over the three sections of the mainsail for three backstay tensions. Tightening the backstay (from #-1 to #+1 in figure), causes the mast to bend and flattens the mainsail. The lowest shrouds oppose the mast bending, hence the highest part of the mast bends more than the lowest part. The *Cp* on the lowest section is not affected by the backstay trim, while the *Cp* on the top section is affected the most. When the mainsail is flattened, the second suction peak, which is due to the sail curvature, decreases.

The best trim depends on the wind conditions. In fact, the second suction peak is located about 40% of the chord, and hence it generates a large side force component and a small thrust force component. When side force or heel moment has to be decreased, the backstay should be tightened. Of course this is common practice in yacht racing.

4.3 Pressures on the Genoa

Figure 8 shows the *Cp* over the three genoa sections for five genoa-sheet trims. Only the *Cp* over the leeward side of the genoa is plotted. For all the trims, the boat was sailed at the same AWA=30°.

In the first trim (#0 in figure), the genoa was trimmed to the *ideal angle of attack* (Theodorsen 1931), which means that the stagnation point is on the leading edge and the suction is entirely due to the profile curvature. This condition is achieved when the genoa luff is close to collapse and it is sailed when the minimum AWA has to be achieved for tactical racing purposes. Tightening the sheet (#+1) causes leading-edge suction peak to occur and a minimum *Cp*=-5 was measured. The increased suction at the leading edge is correlated to a large thrust force component increase. This condition is achieved when the genoa tell-tails are aligned horizontally, and it is sailed when the maximum boat speed has

to be achieved. When the sheet is tightened further (from #+2), the trailing-edge separation point moves upstream until all the sail is fully stalled in trims #+3 and #+4 and all the tell-tails collapse.

Figure 9 shows the *Cp* over the three genoa sections for AWAs=27°, 30°, 45° and 70°. The genoa and the mainsail are trimmed according to the AWA.

On the lowest section, the trends of the leeward *Cp* curves are similar to the trim #+1 in Figure 8, which was the trim that allowed the maximum boat speed. Hence, the genoa was trimmed correctly on the lowest section. On the highest section, the trends of the leeward *Cp* curves are similar to the trim #+0 in Figure 8, which was the trim that allowed the minimum AWA to be sailed. Hence, the genoa was under-trimmed on the highest section. If the genoa twist was decreased, for instance by moving the car, the angle of attack of the highest section would have increased. Lower pressures would have been achieved at the leading edge followed by a pressure recovery, as shown by the lowest section. The systematic error in the genoa trim is partially due to the unfavorable sheeting angle at large AWAs. In fact when the AWA increases, the car should be moved forward and away from the centerline. On the yacht *Aurelie* the car can be moved only forward and backwards. Hence, it cannot be properly trimmed for large AWAs. At AWA=27° and 30°, the over-twist of the genoa is due to a wrong trim; the car should have been moved a little further. At AWA=45° and 60°, the over-twist of the genoa is due to the impossibility to properly trim the car at large AWAs. As a consequence, the larger the AWA the more the top section is under-trimmed and the higher is the pressure on the leeward side.

The leeward-side pressure also increases on the lower section when the AWA increases, because the sail section becomes deeper and deeper, and the trailing edge separation point moves forward.

In conclusion, the pressure load on the genoa decreases significantly when the AWA increases. This is due to the unfavorable sheeting angle which leads to an over-twist on the top sections and to excessively deep lower sections.

5. Conclusions

The present paper shows pressure distributions on a full-scale genoa and mainsail. The paper shows how the pressure distributions change with the sail trim and with the apparent wind angle. These trends can be used to validate the numerical codes that are commonly used in the sail design practice. Moreover, the value of pressure measurements to help understand and optimize sail trims is pointed out.

The pressure coefficients and the related flow field over a generic genoa and mainsail section are shown in the form of a schematic diagram. The pressure coefficient on the windward side of the sails is almost 1.0 over the whole section due to low speed of the flow. On the leeward side, the pressure coefficient shows a suction peak first, followed by a pressure recovery at around 10% of the sail chord, which is related to the turbulent reattachment after the laminar separation bubble. Then a second suction peak occurs due to the sail curvature, followed by a pressure recovery and, eventually, by a pressure plateau due to the trailing edge separation.

In particular, the following conclusions can be drawn from the pressure distributions on the mainsail:

- The mainsail sheet primarily affects the leading-edge suction peak. Tightening the sheet causes the leading-edge suction peak to increase, while the second suction peak due to the sail curvature is not affected significantly.

- The mainsail twist primarily affects the trailing edge separation. Decreasing the twist causes the angle of incidence of the highest sections to increase, which causes the suction to increases until the trailing edge separation becomes excessive.

- The gap between the genoa and the mainsail must be trimmed with care. In fact, a small gap increases the pressure on the leeward side of the mainsail, while a large gap causes the mainsail to stall.

- The camber of the mainsail (trimmed with the backstay tension) primarily affects the second suction peak, which is due to the section curvature. Hence, a larger camber allows a larger suction but it increases the side force component more than the thrust force component.

The pressure distribution on the genoa showed two possible genoa trims. When the genoa is trimmed at the ideal angle of attack, only one suction peak is present and the suction is all due to the sail curvature. This trim allows the lowest apparent wind angle to be sailed. When the genoa is slightly over-trimmed, a leading-edge suction peak occurs and the maximum drive force is achieved. This trim allows the maximum boat speed to be achieved.

When large AWAs are sailed, the unfavorable genoa sheeting angle leads to an excessive twist and to deeper bottom sections. As a consequence, the top sections are under-trimmed and the bottom sections show large trailing edge separation, which lead to a reduced suction on the sail.

6. Acknowledgments

The support of staff and students in the YRU is gratefully acknowledged in helping to carry out the full-scale pressure measurements and to sail *Aurelie*.

7. References

Abbot I.H. & Von Doenhoff A.E. 1049 *Theory of Wing Section*. Dover Publications Inc, New York (ISBN: 0-486-60586-8).

Crompton M.J. & Barret R.V. 2000 *Investigation of the Separation Bubble Formed Behind the Sharp Leading Edge of a Flat Plate at Incidence*. In the proceedings of the Institution of Mechanical Engineers, Part G: Journal of Aerospace Engineering (ISSN 0954-4100), Vol. 214, (3), pp. 157-176.

Flay R.G.J. & Millar S. 2006 *Experimental Consideration Concerning Measurements in Sails: Wind Tunnel and Full Scale.* In the proceedings of the 2nd High Performance Yacht Design Conference (HPYDC2), February 14th-16th, Auckland, New Zealand.

Gaves W., Barbera T., Broun J.B., Imas L. 2008 *Measurements and Simulation of Pressure Distribution on Full Size Scales*. In the proceeding of the 3rd High Performance Yacht Design Conference (HPYDC3), December 2nd-4th, Auckland, New Zealand.

Gentry A. 1971 *The Aerodynamics of Sail Interaction*. In the proceedings of the 3rd AIAA Symposium on the Aero/Hydronautics of Sailing, November 20th, Redondo Beach, California, USA.

Gentry A. 1988 *The Application of Computational Fluid Dynamics to Sails*. In the proceedings of Symposium on Hydrodynamic Performance Enhancement for Marine Applications, October 31st – November 1st, Newport, Rhode Island, USA.

Puddu P., Erriu N., Nurzia F., Pistidda A., Mura A. 2006 *Full Scale Investigation of One-Design Class Catamaran Sails*. In the proceeding of the 2nd High Performance Yacht Design Conference (HPYDC2), February 14th-16th, Auckland, New Zealand.

Marchaj C.A. 1964 *Sailing Theory and Practice*, Adlard Coles Limited, London, England.

Richards P.J. & Lasher W.C. 2008 *Wind Tunnel and CFD Modelling of Pressures on Downwind Sails*. In proceedings of the 6th International Colloquium on Bluff Bodies Aerodynamics & Applications (BBAAVI), July 20th-24th, Milan, Italy.

Skene, N. 1938 *Elements of Yacht design*. Kennedy Bros, New York, USA.

Theodorsen T. 1931 *On the Theory of Wind Sections with Particular Reference to the Lift Distribution*. NACA report number 383.

Thwaites B. 1969 *Incompressible Aerodynamics*, Dover Publications Inc., New York (ISBN: 0-486-65465-6).

Viola I.M. & Flay R.G.J. 2010(a) *Force and Pressure Investigation of Modern Asymmetric Spinnakers*. Journal of Small Craft Technology (RINA), in press.

Viola I.M. & Flay R.G.J. 2010(b), *Pressure Distributions on Modern Asymmetric Spinnakers*. Journal of Small Craft Technology (RINA), submitted.

Warner E.P. & Ober S. 1925. *The aerodynamics of Yacht Sails*. In the proceedings of the 3rd general meeting of the Society of Naval Architects and Marine Engineers, November 12th-13th, New York, USA.

Wilkinson S. 1984 *Partially Separated Flows Around 2D Masts and Sails*, PhD Thesis, University of Southampton, England.

Wilkinson S. 1989 *Static Pressure Distribution over 2D Mast/Sail Geometries*. Journal of Marine Technology, Vol. 26, (4), pp. 333–337.

Wilkinson S. 1990 *Boundary–Layer Explorations Over a Two–Dimensional Mast/Sail Geometry*, Journal of Marine Technology, Vol. 27, pp. 250-256.

Table 1
Specifications of Sparkman and Stephens 24-foot.

Length overall	7.3 m
Length at waterline	5.8 m
Max beam	2.3 m
Max draft	1.3 m
Displacement	2105 kg
Lead keel	862 kg
Mainsail area	13 m^2
Genoa area	13 m^2

Table 2
Specifications of the sails.

	Mainsail	Genoa
1/8th **(of the luff) Girth**	580	350 mm
3/4th **(of the luff) Girth**	1000	660 mm
1/2th **(of the luff) Girth**	1620	1395 mm
1/4th **(of the luff) Girth**	2160	2285 mm
Foot length	2550	3280 mm
Luff length	8060	8800 mm
Leach length	8400	8560 mm
Draft (indicative)	40	48% of the chord
Max camber (indicative)	12	18% of the chord

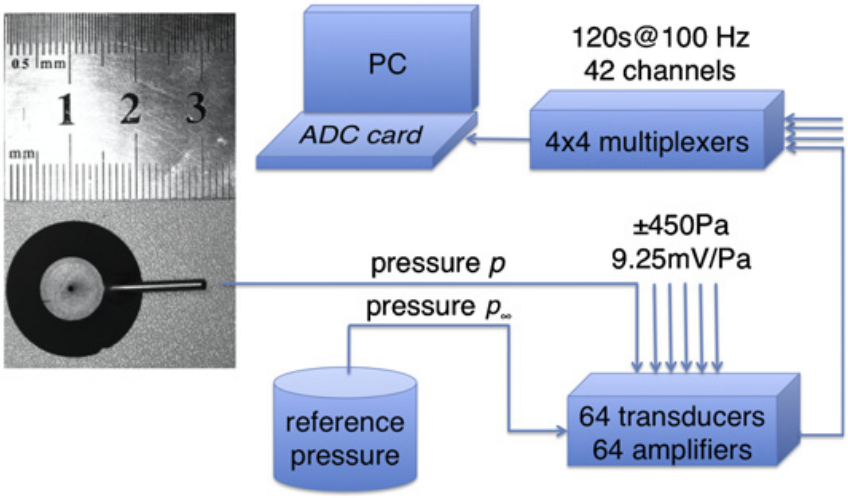

Fig. 1. Schematic diagram of the data acquisition system.

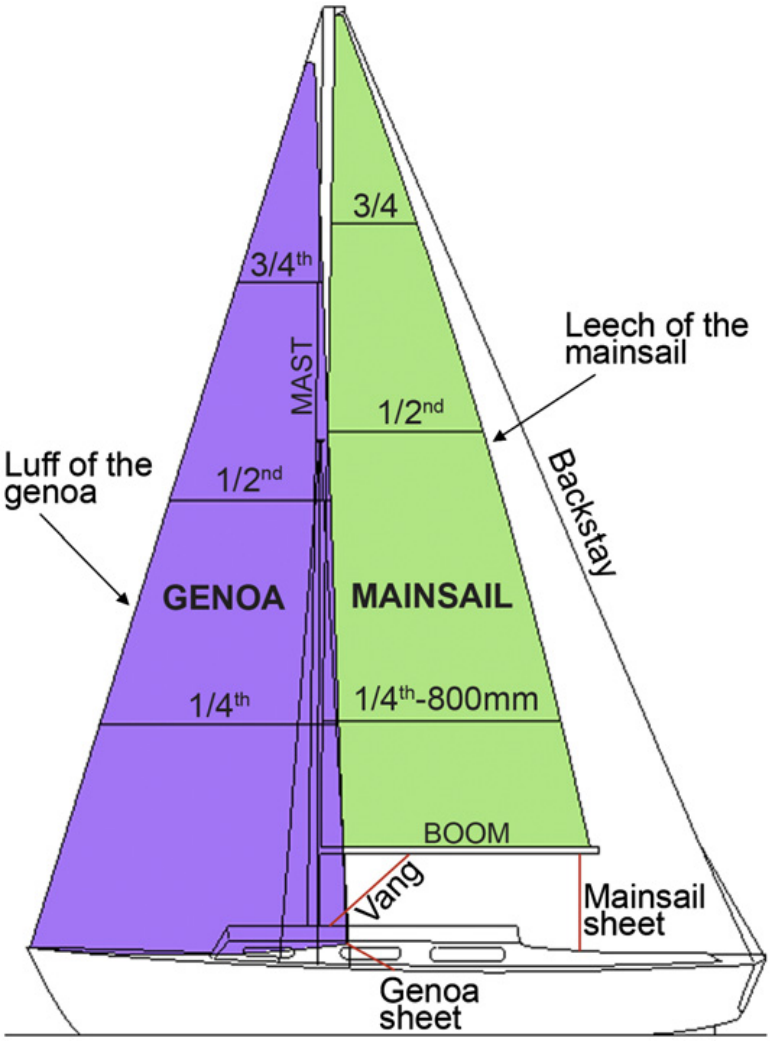

Fig. 2. Sailplan of Sparkman and Stephens 24-foot.

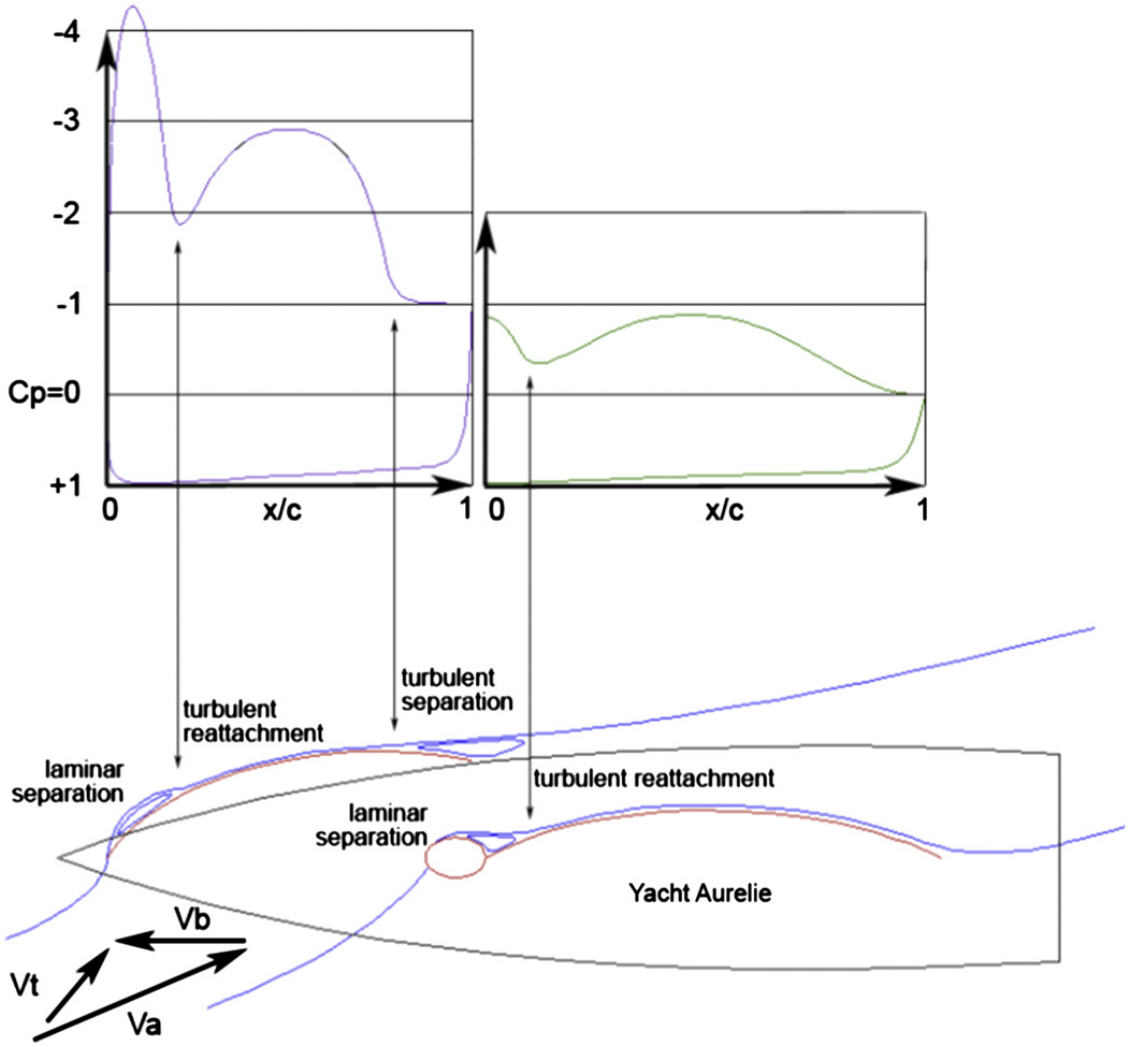

Fig. 3. Schematic diagram of the pressure distributions over the genoa and the mainsail, and the corresponding flow field.

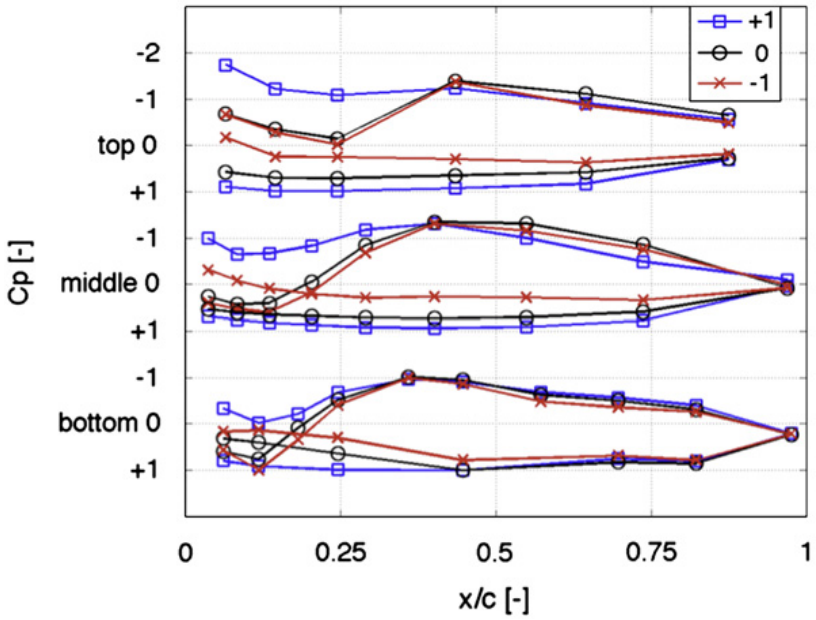

Fig. 4. C_p over the mainsail for 3 mainsail sheet trims.

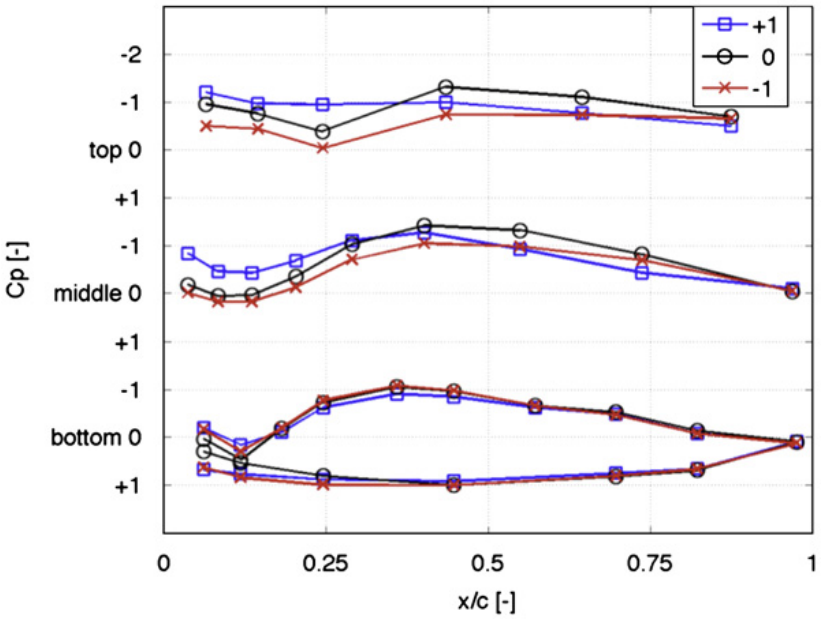

Fig. 5. C_p over the mainsail for 3 mainsail leech tensions.

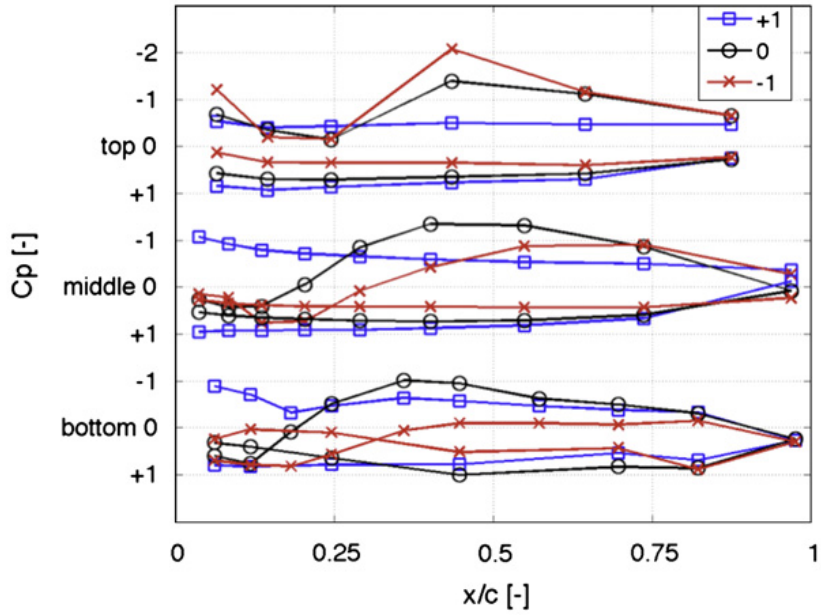

Fig. 6. C_p over the mainsail for 3 genoa/mainsail gap amplitudes.

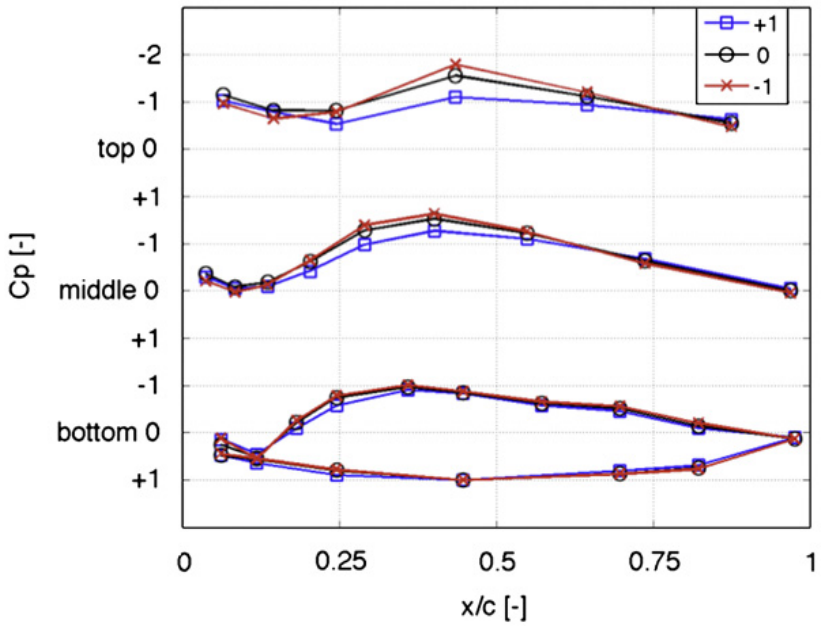

Fig. 7. C_p over the mainsail for 3 backstay trims.

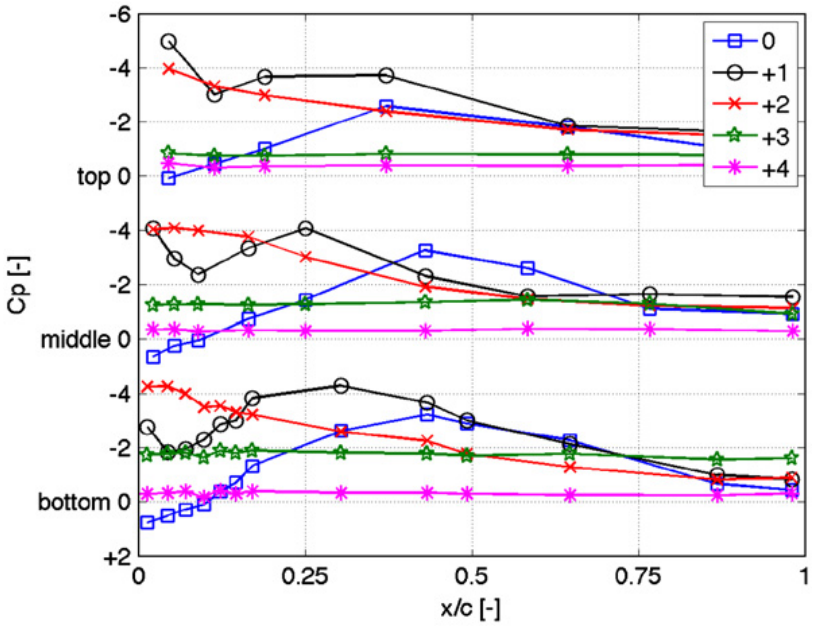

Fig. 8. C_p over the genoa for 5 genoa-sheet trims.

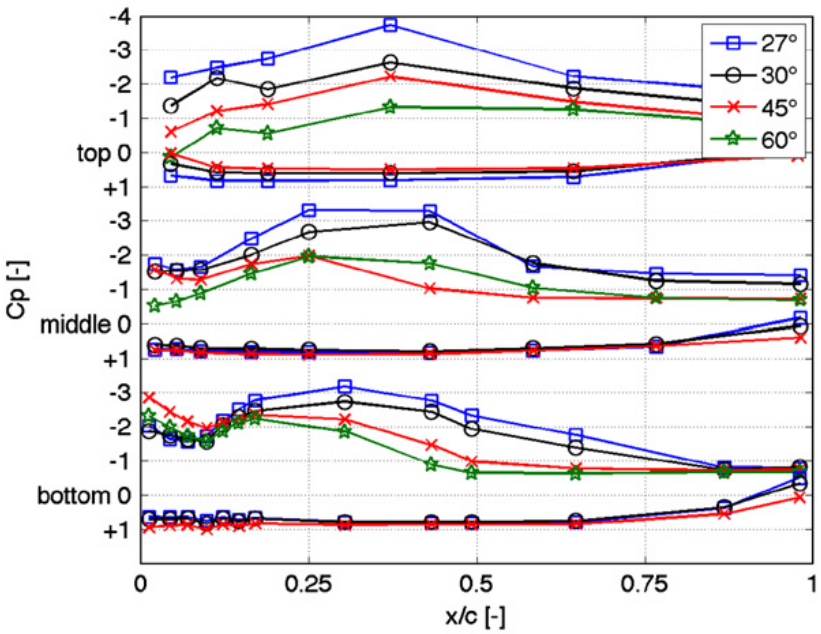

Fig. 9. C_p over the genoa for 4 AWAs.